DEVELOPMENTAL BIOLOGY **191,** 243–258 (1997)
ARTICLE NO. DB978711

Cellular Mechanism Underlying Neural Convergent Extension in *Xenopus laevis* Embryos

Tamira Elul,*,† M. A. R. Koehl,‡ and Ray Keller†

**Biophysics Graduate Group and ‡Department of Integrative Biology, University of California, Berkeley, California 94720; and †Department of Biology, University of Virginia, Charlottesville, Virginia 22903*

Convergent extension, the simultaneous narrowing and lengthening of a tissue, plays a major role in shaping and patterning the neural ectoderm in vertebrate embryos. In this paper, we characterize the cellular mechanism underlying convergent extension of the neural ectoderm in the *Xenopus laevis* late gastrula and neurula embryo. Neural ectoderm in *X. laevis* consists of two components, a superficial layer of epithelial cells overlying deep mesenchymal cells. To investigate the force contribution of the deep cells to convergent extension, we explanted single layers of neural deep cells from late gastrula stage embryos. These "neural deep cell explants" undergo active convergent extension autonomously, implying that these cells contribute force for neural convergent extension *in vivo*. Using time-lapse videorecording of these explants, we observed the neural deep cell behaviors (previously hidden behind an opaque epithelium) underlying convergent extension. We show that neural deep cells mediolaterally intercalate to form a longer, narrower tissue and that cell shape change and cell division contribute little to their convergent extension. Moreover, we characterize the neural deep cell motility driving mediolateral intercalation, also using time-lapse videorecordings. Analyses of these videos revealed that, on average, neural deep cells exhibit mediolaterally biased protrusive activity which is expressed in an episodic fashion. We propose that neural deep cells accomplish mediolateral intercalation by applying their protrusions upon one another, exerting traction, and pulling themselves between one another. This mechanism is similar to that previously described for convergent extension of the mesodermal cells. However, because the neural deep cells do not mediolaterally elongate during their convergent extension as the mesodermal cells do, we predict that a given intercalation will result in more extension for neural deep cells than for the mesodermal cells. Intercalation of neural cells also likely occurs in a more episodic manner than that of the mesodermal cells because the neural cells' mediolateral protrusive activity is episodic, whereas the protrusive activity of mesodermal cells is more continuous. These differences in protrusive activity and cell shape changes between the neural and mesodermal regions may reflect specializations of the same basic mechanism of mediolateral intercalation, tailored to accommodate other aspects of patterning and development of each tissue. These descriptions of the active cell motility underlying neural convergent extension in *X. laevis* are the first high-resolution video documentation of protrusive activity driving neural convergent extension in any system. Our findings provide an important step in the investigation of neural convergent extension in *X. laevis* and further our understanding of convergent extension in general.

INTRODUCTION

In this paper, we investigate the cellular mechanism of convergent extension of the neural ectoderm, the prospective central nervous system tissue, in the late gastrula embryo of the frog *Xenopus laevis*. Convergent extension is a tissue shape change occurring during embryonic development of many metazoan organisms, including flies (Condic *et al.*, 1991; Irvine and Wiechaus, 1994), echinoderms (Ettensohn, 1985; Hardin and Cheng, 1986), amphibians (Jacobson, 1981; Keller and Danilchik, 1988), and fish (Trinkaus *et al.*, 1992; Warga and Kimmel, 1990), in which a tissue narrows along one axis while elongating along a perpendicular axis. Convergent extension of the neural ectoderm is an important morphogenetic process in generating the vertebrate body plan. During convergent extension the neural tissue, which is initially very short anteroposteriorly and very wide mediolaterally, lengthens along the anteroposterior axis and narrows mediolaterally (Jacobson and Gordon, 1976; Keller *et al.*, 1992a). In amphibians and avians conver-

0012-1606/97 $25.00

gent extension has been shown to play a major role in neurulation (Jacobson, 1978, 1981; Jacobson and Moury, 1995; Jacobson *et al.*, 1986; Keller *et al.*, 1992b; Schoenwolf and Alvarez, 1989). Moreover, convergent extension of the neural ectoderm is important in the patterning of this tissue by the mesoderm (reviewed in Gould and Grainger, 1997). The fact that the neural tissue is initially very short anteroposteriorly means that early planar inductive signals from the mesoderm originating at the posterior end of the neural tissue, or early vertical signals from the involuted mesoderm tissue, can easily reach anterior neural tissue (Keller *et al.*, 1996, 1992b; Nieuwkoop and Florshutz, 1950; Poznanski and Keller, 1997).

Although several cell behaviors are involved in neural convergent extension in vertebrates, including cell division and cell shape change, cell rearrangement is the major and consistent contributor to this process in all vertebrates. In amphibians, neural cells rearrange (intercalate) to form a longer, narrower array during convergent extension (Jacobson, 1978; Jacobson and Gordon, 1976; Keller *et al.*, 1992a). Change in cell shape (columnarization) also occurs during convergent extension (Burnside and Jacobson, 1968); although such columnarization may narrow the tissue, it does not produce extension in amphibians (Jacobson and Gordon, 1976). Although cell division occurs in the amphibian neural ectoderm during convergent extension (Hartenstein, 1989), inhibitors of cell division do not affect normal neural morphogenesis (Harris and Hartenstein, 1991). In avians neural convergent extension involves cell rearrangement and oriented cell division, while cell shape change counters the extension produced by cell rearrangement (Schoenwolf and Alvarez, 1989; Schoenwolf and Yuan, 1995). Recent studies have indicated that cell rearrangement also contributes to neural convergent extension in fish; while change in cell shape occurs, it does not in itself produce convergent extension (M. Cooper, personal communication).

Although cell rearrangement is the one universal component of neural convergent extension in the vertebrates studied thus far, the mechanism by which the cells rearrange is not known. Jacobson and his associates argue that cells in the newt neural plate are captured at the notoplate–neural plate and the neural plate–epidermal boundaries, thus elongating these boundaries and producing convergent extension (Jacobson, 1981; Jacobson and Moury, 1995; Jacobson *et al.*, 1986). Although protrusions have been observed on neural epithelial cells in fixed newt neural plates (Jacobson *et al.*, 1986), the protrusive activity that brings about cell rearrangement has not been observed in live tissues of this system or any of the other systems mentioned above.

The cell motility that drives rearrangement has been extensively described in only one system, the convergent extension of the dorsal mesoderm tissue in *X. laevis* (Shih and Keller, 1992a; Shih and Keller, 1992b). In this case, the mesoderm tissue undergoes autonomous convergent extension by mediolateral cell intercalation (Shih and Keller, 1992a). High-magnification time-lapse videomicroscopy showed that these mesodermal cells develop bipolar, mediolaterally oriented protrusive activity, which is thought to exert traction on adjacent cells and pull the cells between one another (Shih and Keller, 1992a). Since this is the only example of cell motility during cell intercalation that has been described, it is not known if this mechanism is unique to the mesoderm or if it is a common or perhaps a universal mechanism. Thus it is important that we determine the protrusive activity underlying neural cell intercalation.

Given the fundamental nature of convergent extension in morphogenesis and in neural development, and the little that is known about its mechanism, we undertook to resolve the cellular mechanism underlying neural convergent extension in *X. laevis*.

In the *X. laevis* late gastrula embryo, the neural ectoderm consists of a layer of epithelial cells overlying a layer of deep cells (Keller, 1975, 1976, 1978). The neural tissue overlies the dorsal mesoderm tissue, and these two tissues undergo convergent extension together during the late gastrula and neurula stages (stages 11–20). Neural ectoderm undergoes convergent extension autonomously in a Keller sandwich explant (consisting of deep cells sandwiched between two layers of epithelial cells), requiring only planar contact with the mesoderm up to the late gastrula stage in order to do so (Keller *et al.*, 1992b; Keller and Tibbetts, 1989). Mediolateral intercalation of both the neural epithelial and deep cells is a major and essential component of convergent extension of both these layers of neural tissue (Keller *et al.*, 1992a; Keller, 1978). It is not known whether the neural epithelial cells, the neural deep cells, or both generate force for convergent extension. Furthermore, the protrusive activity driving the cell intercalation in the force-producing layer or layers of the neural tissue has not been described.

In this paper, we show that neural deep cells can undergo convergent extension autonomously. Using time-lapse videomicroscopy of neural deep cells in explants we observe that neural deep cells actively mediolaterally intercalate during convergent extension. We calculate that this intercalation largely accounts for the extension of these explants, and we show that cell shape change and cell division contribute very little to convergent extension. Moreover, we resolve the motility of neural deep cells during mediolateral intercalation, using time-lapse videomicroscopy of fluorescently labeled cells in explants. We show that these cells have mediolaterally biased protrusive activity which is expressed in an episodic fashion. We propose that this mediolateral protrusive activity drives mediolateral intercalation of neural deep cells by a mechanism similar to that exhibited by mesodermal cells. These results are an important step in our understanding of neural convergent extension in *X. laevis* and of convergent extension in general.

MATERIALS AND METHODS

Embryo and Explant Preparation

Eggs were fertilized and dejellied by standard methods (Kay and Peng, 1991). Fluorescent labeling of 32 cell embryos was performed

as described below. Embryos were then held at 16°C in one-third strength modified Barth's solution (MBS) (Gurdon, 1977). Shortly before use, embryos were transferred to modified Danilchik's solution (DFA) (Sater *et al.,* 1993) plus bovine serum albumin (BSA, 1 g/ml) and moved to a cold plate for microsurgery (15° ± 1°C). DFA mimics amphibian blastocoel fluid in composition and supports normal deep cell behavior (Shih and Keller, 1992a). BSA coats glass and plastic, thereby reducing adhesion and friction between explants and cover glass (Keller, 1991). Embryos were staged according to Nieuwkoop and Faber (1967).

Explants were made from stages 11.5 to 12 late gastrula embryos, using eyebrow hair knives and hairloops. The neural ectoderm epithelium was removed and discarded and the remaining dorsal tissues of the embryo—the deep layers of the neural ectoderm, the mesoderm, and the endodermal epithelium—were explanted, as diagramed in Fig. 1. The mesoderm and endoderm were then sheared off, leaving a single layer of neural ectoderm deep cells. We call such an explant a ''neural deep cell explant.''

Fluorescent Labeling

In order to enhance resolution of cell outlines and protrusive activity, a dispersed population of neural cells was fluorescently labeled. Embryos were tipped and marked prior to the first cell cleavage to facilitate identification of the dorsal side of the embryo (Kay and Peng, 1991). At the 32-cell stage, 20 nl of RD-G or -A (rhodamine dextran green or amine, Molecular Probes) was injected with a pressure injector into dorsal blastomere ''B1.'' Mixing between B1 progeny and progeny of neighboring uninjected blastomeres resulted in the desired scattered population of fluorescently labeled cells at the late gastrula stage.

Time-Lapse Videomicroscopy

Epiillumination. Explants were illuminated with low-angle fiber optics and imaged with a Hammamatsu C-2400 CCD (XC-77) camera. For lower magnification videos, an Olympus Provis microscope and a X4 fluor objective was used. Images were taken once every 5 min and recorded to a Pentium computer. Summing of frames and contrast enhancement was performed by Metamorph image processing software (Version 2, Universal Imaging, Brandywine, PA). For higher magnification videos, a Nikon inverted DIAPHOT-TMD microscope and a X10 fluor objective were used. Images were taken once every 60 sec and recorded to an optical disk (Panasonic OMDR TQ-2028F). Summing of frames and contrast enhancement was performed by Image-1 image processing software (Version 3.65, Universal Imaging).

Epifluorescence illumination. Explants were illuminated with a variable intensity halogen lamp and imaged with a Hammamatsu C2400-08 SIT camera. Epifluorescence illumination was regulated by a Uniblitz electronic shutter (Vincent Associates, PA) controlled by the image processing software to occur only during summing of frames. Images were taken once every 60 sec. For lower magnification videos, a Nikon inverted DIAPHOT-TMD microscope and a X20 fluor objective were used. Summing of frames and contrast enhancement was performed by Image-1 and images were recorded to the optical disk. For higher magnification videos, an Olympus inverted IX70 microscope and a X40 fluor objective were used. Summing of frames and contrast enhancement of images was performed by Metamorph and images were recorded to the computer.

Morphometric and Kinematic Measurements

Explant dimensions and cell dimensions, surface areas, and orientations were measured from videorecordings using Image-1, Metamorph, or NIH Image (Version 1.60) image processing software. Statistics were performed using Statview software (Version 4.5). The Mann–Whitney nonparametric statistical test was used to test for significance of differences except in the case of angular distributions of protrusions (see below).

Extension rates for explants were calculated by measuring the anteroposterior extent of the explant originally and at a later time. The difference between these measurements was divided by the original anteroposterior extent of the explant and the time elapsed to yield an extension rate. Similarly, convergence rates for explants were calculated by measuring the maximum mediolateral extent of an explant originally and at a later time. The difference between these measurements was divided by the original mediolateral extent of the explant and the time elapsed to yield a convergence rate.

Length-to-width ratios (L/W) of cells were calculated by measuring the length of the long axis of a cell (''length'') and of the axis perpendicular to it (''width''). Mean L/W for independent samples of 5 or more cells in an explant were calculated at different times during convergent extension from lower magnification epifluorescence videos (Fig. 5). Mean surface areas were calculated for samples of 20 or more cells at two different times during convergent extension from higher magnification epiillumination videos.

The *mediolateral intercalation index* was calculated as described in Shih and Keller (1992a). Briefly, a continuous column of cells lying parallel to the anteroposterior axis was identified. These identified cells were traced to a later stage by time-lapse recording and then connected to one another by identifying and counting the intervening cells, which have intercalated. This number was added to the original number of cells in the column, and then the total was divided by the original number in the column to give the *mediolateral intercalation index*. The *extension index* is the original distance between cells along the anteroposterior axis divided into the distance between them at a later stage.

Two methods were used to calculate the frequency and angular distribution of protrusions. First, protrusions were inferred from measurements of cell shape changes: The length of the major axis of a cell was measured in 45 consecutive frames in lower magnification epifluorescence videos. This length was then plotted as a function of time (Fig. 7A). A peak-to-trough change greater than 4 μm on such a plot was considered a single episode of cell elongation. A cell's average orientation of major axis was calculated by taking the time-average of the angle of the cell's major axis relative to the mediolateral axis of the explant over 45 consecutive frames (Fig. 7B). Angles between the major axes of cells and the mediolateral axis of the explant were recorded to the nearest 10°. The second more direct method of counting protrusions involved tracing the margin of a cell in consecutive frames (30–150 frames, depending on the cell) from higher magnification epifluorescence videos. Extensions of a cells' margin relative to its outline in the previous frame were considered a protrusion. New or successive advances (or both) of protrusions greater than 3 μm were counted. New advances are advances of protrusions that were inactive in the previous frame while successive advances are advances of protrusions that were active (advanced) in the previous frame. The angular distribution of protrusions was calculated by counting the percent of protrusions falling into each of twelve 30° sectors around a cell's perimeter (Figs. 9 and 10). Rayleigh's test was used to test whether

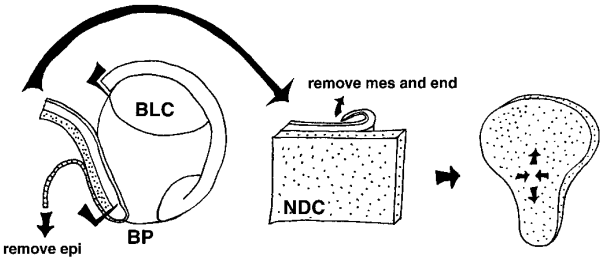

FIG. 1. Schematic diagram shows how neural deep cell explants were made. A sagittal view of a late gastrula stage embryo is shown at left (stage 11.5–12). At this stage the neural epithelium was removed and discarded. The neural deep layer (stippled) together with the mesoderm and endodermal epithelium were then cut out and explanted from the embryo. The cut at the posterior edge of these layers was made above the estimated limit of involution, between the neural and mesodermal tissues, in order to ensure that only neural deep tissue would be present on one side of the explants. The mesoderm and endodermal epithelium were then removed from the underside of the neural deep cells and discarded (center image). The remaining layer of neural deep cells underwent convergent extension, narrowing mediolaterally and elongating anteroposteriorly. BLC, blastocoel; BP, blastopore; NDC, neural deep cells; epi, epithelium; mes, mesoderm; end, endoderm.

the angular distributions of protrusions were significantly different from a uniform distribution (Zar, 1974).

Cell Division

The percent of cells dividing was calculated by dividing the number of fluorescently labeled cells that divided in the duration of the video by the number of fluorescently labeled cells visible initially. This number was then divided by the time of the video to yield a rate of cell division.

Antibody Staining

Antibody staining was performed on explants in order to assay their tissue composition. An N-CAM monoclonal antibody, 6f11 (Harris and Hartenstein, 1991), was used to stain the explants for neural tissue. The monoclonal antibodies Tor-70 (Bolce *et al.,* 1992; Kushner, 1984) and 12-101 (Kintner and Brockes, 1984), which are specific for notochord and somites, respectively, were used to stain these explants for mesodermal tissues. The fixation and staining protocol was the same as that used by Domingo and Keller (1995).

RESULTS

Neural Deep Cell Explants Consist of Neural Ectoderm with Negligible Mesodermal Contamination

In order to determine whether neural deep cells converge and extend autonomously and to investigate the cell behaviors that underlie their convergent extension, we isolated the neural deep cells in single layer explants taken from late gastrula *X. laevis* embryos (stages 11.5–12) (Fig. 1). Before analyzing cell behaviors in these neural deep cell explants, we used antibodies to mesodermal and neural markers to confirm that the explants consisted mainly of neural tissue and that mesodermal contamination was minimal. The adhesion between the neural deep and involuted mesodermal tissue layers is very strong by stage 11.5, especially in the medial region of the tissues between the notoplate and notochord. Moreover, the limit of involution between the posterior neural tissue and noninvoluted mesodermal tissue is not apparent at stage 11.5. Therefore, it was possible that we had not removed all the involuted and noninvoluted mesodermal cells from our explants. All seven explants that we stained with antibodies, however, consisted mainly of neural tissue and contained a very small number of mesodermal cells. The mesodermal staining occurred in one of two patterns. Three of the seven explants contained a few dispersed mesodermal cells (15 mesodermal cells stain in Fig. 2A), while in the remaining four explants, the mesodermal cells were found in a few small clumps (three clumps or about 10 cells stain in Fig. 2B). Occasionally a clump was organized into notochord, as indicated by the short arrow in Fig. 2B. The mesodermal staining was most often scattered over the explants and not localized to the posterior edge, indicating that involuted rather than noninvoluted mesodermal tissue is the more common source of contamination.

These results argue strongly that we did not video mesodermal cells and incorporate them into our data on neural cell behaviors. We estimate that less than 10% of the neural deep cell explant area contained contaminating mesodermal cells. Moreover, the contaminating cells were mainly involuted mesoderm, and thus they were located on the side of the explant opposite to the side that we observed in our time-lapse videos. Finally, the morphology of neural deep cells and mesodermal cells differs at the stages during which we observe cell behaviors (see below); indeed, we rejected any explants that contained obvious mesodermal cells.

Neural Deep Cells Converge and Extend Autonomously

Neural deep cell explants converged and extended autonomously during the neurula stages (stages 13 to 22), independent of any physiological or mechanical contact with neighboring tissues. Convergent extension varied in the different regions of the explants; the medial-posterior regions of these explants narrowed and lengthened significantly and consistently, and the more lateral-anterior regions also narrowed and lengthened in some explants (Figs. 3A, 3C, and 3D). This posterior region of neural deep cell explants that consistently undergoes convergent extension corresponds to prospective hindbrain and spinal cord tissue (Eagleson and Harris, 1990; Keller *et al.*, 1992a).

In videos of these neural deep cell explants, we observed that a small posterior or medial region within each explant appeared to undergo most of the convergent extension. We

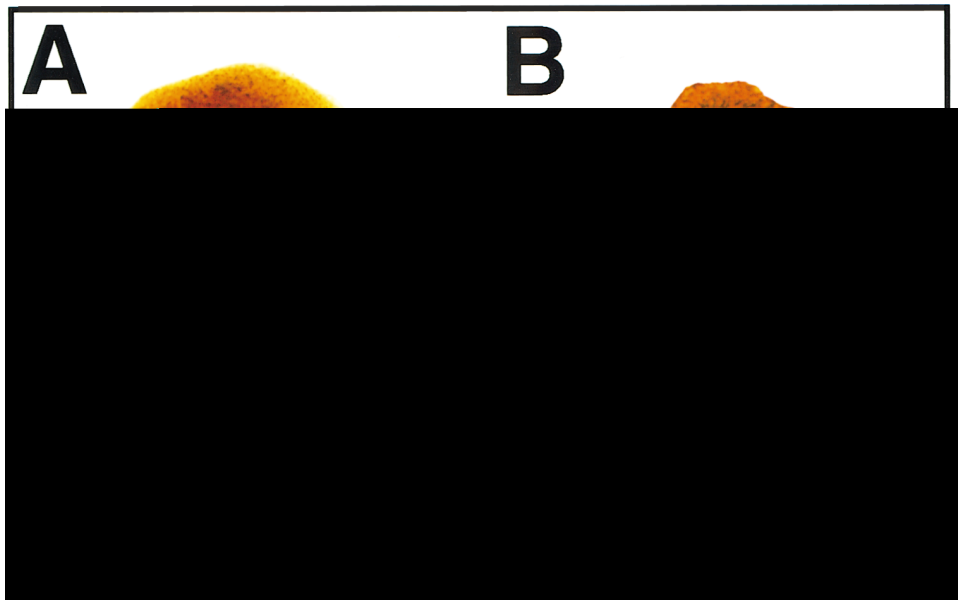

FIG. 2. Photographs show neural deep cell explants at stage 20, stained with antibodies to N-CAM (orange) and to notochordal and somitic mesoderm (brown). Most of the explant areas were neural tissue, although all explants contained a small number of contaminating mesodermal cells; some explants contained a few scattered mesodermal cells (arrow, A); others contained small patches of mesoderm (long arrow, B), including occasionally a patch organized into notochord (small arrow, B).

confirmed this observation by measuring local distortions of areas in neural deep cell explants during convergent extension, using grids superposed on time-lapse videos of explants. A typical grid distortion is shown in Fig. 3B. In this example the 2 medial-most boxes (of 20 boxes total) underwent the most convergent extension. These two boxes actually increased their anteroposterior extent approximately twofold while decreasing their mediolateral extent by a third. (The loss of area in this region is due to slight decrease in cell surface area, see below.)

The fact that a small region within each explant underwent most of the convergent extension led us to make our neural deep cell explants smaller, about 600 μm in mean mediolateral extent and 550 μm in mean anteroposterior extent (as opposed to the original mean dimensions of 1500 μm in mediolateral extent and 700 μm in anteroposterior extent). The increase in the amount of convergent extension in these smaller explants was striking (compare Fig. 3A with Figs. 3C and 3D). The entire anteroposterior extent of these smaller explants narrowed and lengthened significantly (Figs. 3C and 3D). In one especially small explant, the anterior part of the explant narrowed as much as the posterior part (data not shown). Comparisons of rates of convergence and of extension between large and small explants revealed that the main increase was in the rate of convergence (Table 1). The mean rate of extension also increased from 3%/hr in the larger explants to 5%/hr in the smaller explants. Note that these rates of extension are comparable to that measured for the mesodermal shaved explant (explant of deep cells and epithelial cells) (Table 2). However, we should emphasize that even in smaller neural deep cell explants the medioposterior regions undergo the most convergent extension. We calculated the extension rate for the medioposterior most cells of one neural deep cell explant to be about 20%/hr.

These results demonstrate that active convergent extension is autonomous only in the medial region of the neural deep tissue at the late gastrula stage when we make our explants. The most anterolateral tissue of our larger neural deep cell explants cannot autonomously converge and extend at this time and may actually inhibit convergent extension by contributing mechanical resistance or presenting inhibitory signals (Hemmati-Brivanlou and Melton, 1997).

Mediolateral Intercalation Underlies Convergent Extension

Conceivably, a combination of cell rearrangement, cell shape change, and oriented cell division could underlie convergent extension of neural deep cell explants. In order to investigate whether neural deep cells actively rearrange during the convergent extension observed here we traced groups of cells from higher magnification time-lapse videos of explants during convergent extension. One such tracing is shown in Fig. 4, which illustrates the cell behaviors we observed in all three explants that we videoed at this magni-

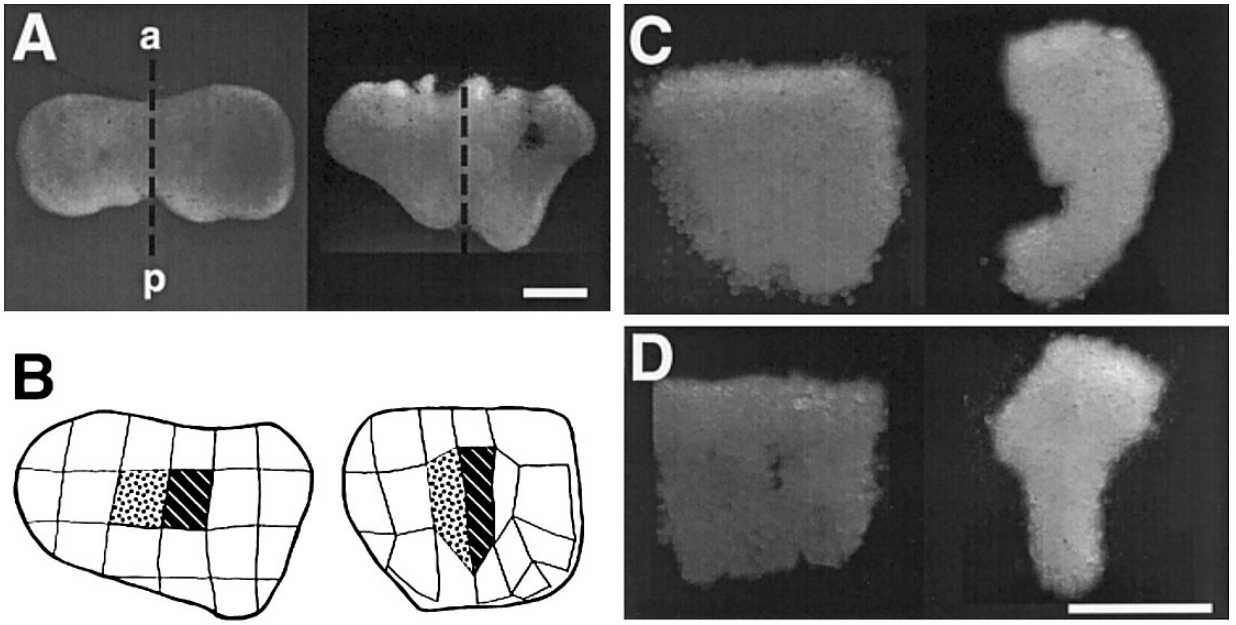

FIG. 3. Four different examples of neural deep cell explants are shown (A–D) before convergent extension, at stage 12 (left column) and after convergent extension, at stage 20 (right column). (A) The posterior region of this large explant converged and extended, narrowing mediolaterally and elongating anteroposteriorly. (B) We performed time-lapse video of a larger neural deep cell explant during convergent extension. A grid was superposed on the explant in the initial frame of the video and cells identifiable by characteristic pigmentation located at the corners of the grid boxes were traced throughout the duration of the video. Note that the anteroposterior extent of each of the two shaded boxes extended almost twofold, while the remaining grid boxes did not distort significantly. (C, D) Two examples of smaller explants are shown: The entire anteroposterior extent of such smaller explants converged and extended, narrowing mediolaterally and elongating anteroposteriorly. The anteroposterior axis is indicated in the first example (A). a, anterior; p, posterior. (C) and (D) are at a higher magnification than (A) and (B). Scale bars represent 400 μm.

fication. The cells shown in this tracing have rearranged such that fewer cells are located along the mediolateral axis, while more cells are located along the anteroposterior axis. For example, the cells shown in blue (numbered 1, 6, 7, 11, 12, and 46) all came to lie on a single meridian. Cells 46 and 1 intercalated between cells 6 and 7, while cell 12 moved posterior to cell 11. Note that another group of cells (shown in yellow) that were initially located on the other side of the midline from the blue cells came to lie on the same meridian as the blue cells at the end of this 100-min period. In the yellow population, cells 62 and 63 intercalated between cells 61 and 75, moving the latter cells apart along the anteroposterior axis. A third group of cells (shown in red) exhibited similar intercalation behavior, also coming to lie on a single meridian. Note that this convergent extension of the tissue, mediated by cell intercalation, occurred mostly in the posterior medial region of the explant (blue, yellow, and red populations). The anterior medial cells (such as those shown in purple) and the lateral cells (such as those shown in green or orange) did not significantly rearrange or

TABLE 1
Summary of Rates of Convergent Extension for Large and Small Neural Deep Cell Explants

Size of explants	Mean initial width (M-L) (μm)	Mean rate of convergence* (%/hr)	Mean initial length (A-P) (μm)	Mean rate of extension (%/hr)	*N*
Large	1456 (355)	1.2 (0.9)	672 (76)	3 (2.3)	7
Small	595 (101)	4.3 (1.2)	535 (71)	5 (2.7)	6

Note. Mean values are shown for all measured parameters, with standard deviations in parentheses. *N*, number or explants.
* Difference between mean rates of convergence for large and small explants was highly statistically significant ($P < 0.005$).

TABLE 2
Summary of Convergent Extension and Cell Behaviors in Neural Deep Cell and Mesoderm Shaved Explants

Type of explant	Extension rate	Mean max L/W	New protrusion rate[a]	Percentage of new protrusions within 30° of mediolateral axis	Cell Division rate
Neural deep cell[b]	4.8 %/hr (2.1 %/hr) [24 explants]	2.18 (0.55) [34 cells; 5 or more cells per explant, 5 explants]	24 per hour (9 per hour) [17 cells; 1 or more cells per explant 4 explants]	48% [17 cells; 1 or more cells per explant, 4 explants]	3%/hr (3.62 %/hr) [4 explants]
Mesoderm shaved[c]	3–7 %/hr	3.2 (0.11)	7 per hr	>70%	2 %/hr

Note. Mean values were calculated for relevant parameters. Standard deviations are shown in parentheses; sample sizes are shown in square brackets.

[a] Protrusion rates include advances of new protrusions in all directions. Protrusion rate for neural cells for mediolaterally oriented protrusions only is 12 per hour (SD = 4 per hour).

[b] Data in this row were compiled from videorecordings of explants during some portion or all of stages 13–20.

[c] Data in this row were taken and calculated from data in Shih and Keller (1992a) or Keller and others (1992c) and represent stages 10.5–12.

converge and extend during this period. The lateral cells, however, were brought closer to the midline by the intercalation of the medial cells (e.g., those shown in blue, yellow, and red).

We also measured shape changes of neural deep cells in explants undergoing convergent extension in order to determine whether they contribute to convergent extension. For cell shape change to contribute to convergent extension, neural deep cells would have to narrow mediolaterally and elongate anteroposteriorly during convergent extension. Alternately, if neural deep cells elongate mediolaterally and shorten anteroposteriorly, as the mesodermal cells do (Shih and Keller, 1992a), they would reduce the amount of convergent extension generated by intercalation. Measurements of mean L/W of neural deep cells at different times during convergent extension, however, argue that neural deep cells do not show such progressive shape changes throughout most of their convergent extension (stages 12–22) (Fig. 5). Neural deep cells are slightly elongated during most of their convergent extension (Table 2), and their long axes tend to be mediolaterally oriented, as described in the next section (Fig. 7B). However, only two of the five explants that we analyzed showed statistically significant changes in mean L/W (Fig. 5A). In these explants cells became more isodiametric toward the end of their convergent extension, which could contribute to convergence but not extension of the explant. The three remaining explants that we analyzed did not show a statistically significant change in mean L/W (Fig. 5B). Moreover, for the cells shown in Fig. 4, the mean surface area decreased by 16% ($P < 0.05$), which again could contribute to convergence but not to extension of the tissue. Thus, although neural deep cells are mediolaterally elongated during convergent extension they do not progressively change shape throughout their convergent extension, as the mesodermal cells do. Note however, that the neural deep cells *episodically* elongate during convergent extension as a result of their protrusive activity, described in detail in the next section.

Finally, we measured the rate of neural deep cell division during convergent extension from time-lapse videos to be 3%/hr (SD = 3.62%/hr, $n = 4$ explants) (Table 2) but no consistent orientation of division was apparent. Moreover, arrays of cells were observed to converge and extend by cell intercalation without any cell division (Fig. 4, e.g., cells shown in blue).

These data suggest that convergent extension of neural deep cell explants occurs primarily by mediolateral intercalation. In order to determine a quantitative value for the contribution of mediolateral intercalation to extension of these explants we calculated the *mediolateral intercalation index* (extension resulting from given intercalation if cells did not change shape) and the *extension index* (actual extension resulting from given intercalation). For the cells in Fig. 4 shown in blue, yellow, and red, we calculated a mean mediolateral intercalation index of 1.48 and a mean extension index of 1.62, confirming that mediolateral intercalation is largely responsible for the extension of these groups of cells.

Neural Deep Cells Exhibit Mediolaterally Biased Protrusive Activity

The neural deep cells converge and extend autonomously by mediolateral intercalation, without the aid of any other cells. In order to do so, they must undergo some form of active motility. Moreover, because mediolateral intercalation is an anisotropic process, their active motility is likely to be anisotropic.

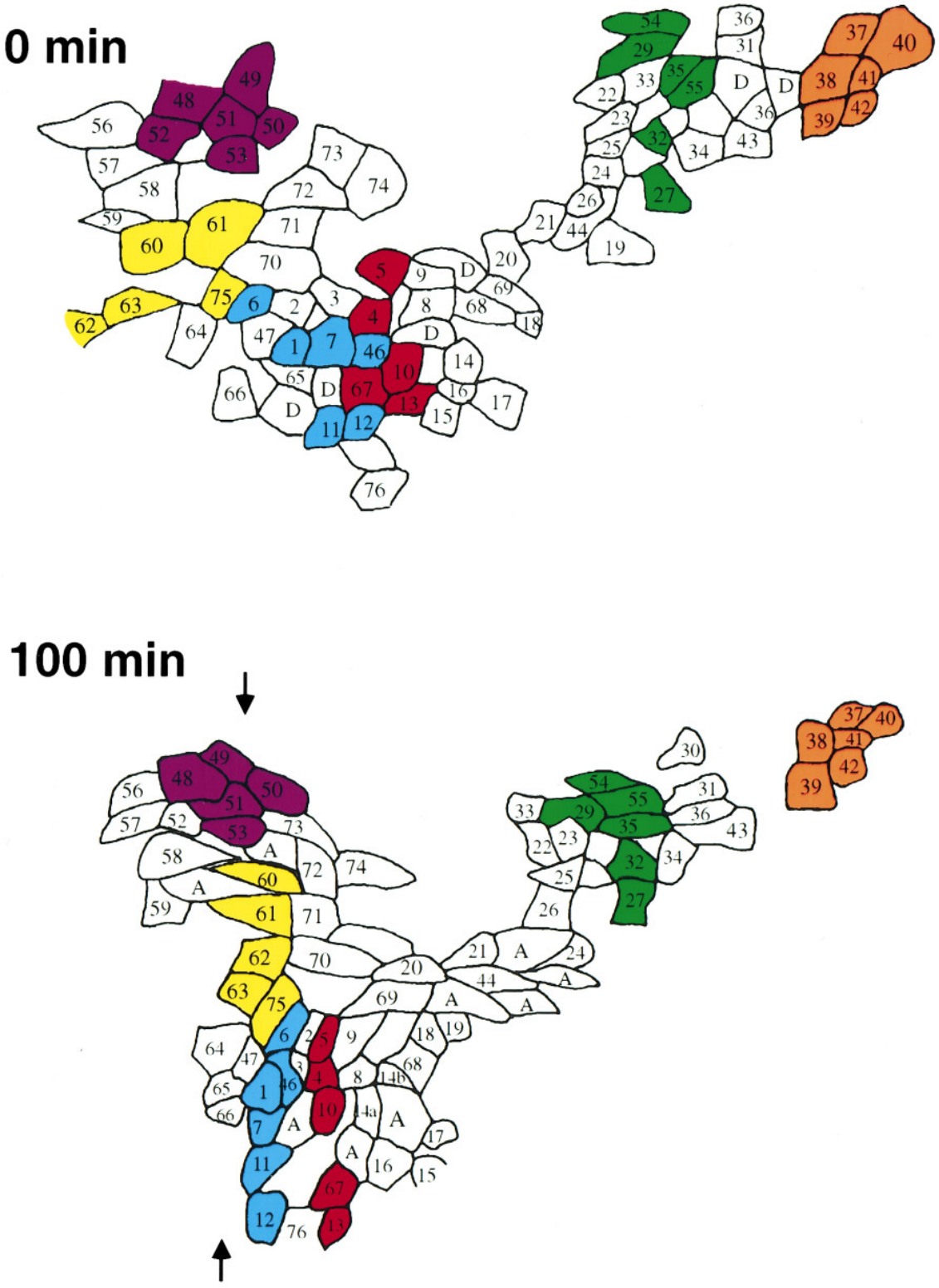

FIG. 4. Tracings of cells from two frames of an epiillumination time-lapse video of a neural deep cell explant shows cell intercalation during convergent extension. Note that the posterior-medial cells (shown in blue, red, and yellow) underwent convergent extension by mediolateral intercalation. The behavior of the colored cell populations is discussed in detail in the text. The approximate midline of the explant is indicated in the lower tracing (arrows).

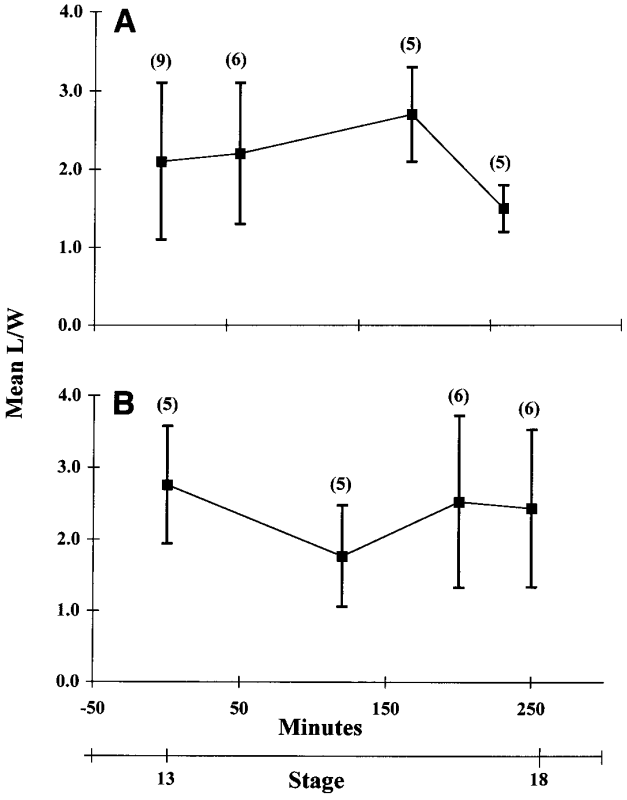

FIG. 5. The mean L/W is shown at different times during convergent extension for two different explants. Each mean represents the average of L/W ratios for 5 or more cells, and the number of cells is indicated above the bars. (A) In this explant the mean L/W at stage 18 is statistically different from that at the previous time point ($P < 0.05$), indicating that cells became more isodiametric at stage 18. (B) In this explant, there is no statistically significant difference between the stages. Maximum mean L/W were selected from each of these plots and averaged with the maximum mean L/W for other explants to yield the mean maximum L/W, shown in Table 2. Error bars indicate one standard deviation.

To observe the motility of neural deep cells we made time-lapse videos (×30) of fluorescently labeled cells in explants undergoing convergent extension. These videos revealed that the neural cells episodically elongate and shorten as they intercalate (Fig. 6). The episodic cell shape changes observed at this magnification likely reflect extension and retraction of protrusions (though not necessarily of a single protrusion). Measurements of the lengths of neural cells' major axes exhibited corresponding episodic increases and decreases, confirming these video observations (Fig. 7A). We calculated a rate for episodes of elongation for neural deep cells of 5 per hour (SD = 1/hr, $n = 5$ cells per explant, three explants). Moreover, plots of neural deep cells' major axis showed them generally to be mediolaterally oriented, as illustrated by the cell in Fig. 7B whose time-averaged orientation of long axis is 10° from the mediolateral axis of the explant (range from −30 to +30 degrees). The mean of such time-averaged angles was 6° (SD = 12.2°, $n = 5$ cells per explant, three explants). This analysis shows that, on average, neural deep cells episodically elongate and shorten in the mediolateral orientation. Interpreting these episodes of elongation and shortening to reflect protrusive activity, these data further suggest that neural deep cells exhibit mediolaterally oriented protrusive activity.

Inferring protrusions from cell shape changes, however, is not as convincing a demonstration of protrusive activity as a direct count of protrusions would be. Moreover, our analysis did not indicate whether neural deep cells exhibit anisotropic protrusive activity, that is, more protrusive activity proportionately in the mediolateral orientation than in other orientations. In order to further examine neural deep cells' protrusive activity we enlarged our previous time-lapse videos and made new higher magnification (×60) time-lapse videos of fluorescently labeled cells in explants undergoing convergent extension. Analyses of these videos confirmed that neural cells tend to have dominant lamelliform and filiform protrusions oriented mediolaterally (Fig. 8). We also discovered that while neural cells advance and retract these mediolateral protrusions they continuously extend and retract numerous small triangular, filiform, and

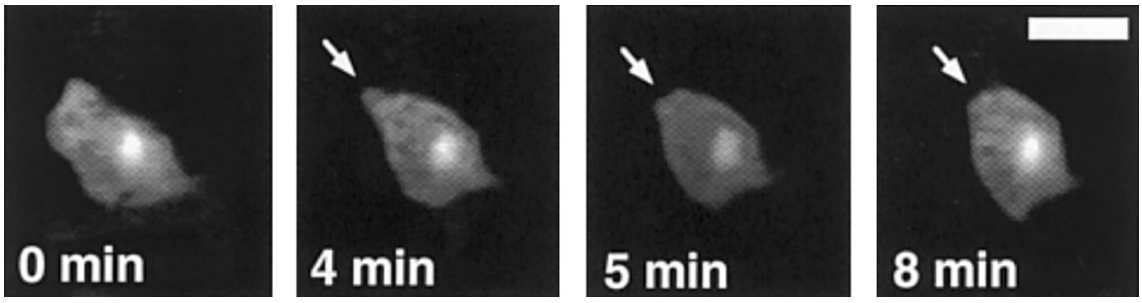

FIG. 6. Stills taken from a time-lapse video (×30) show sequential images of a cell in a neural deep cell explant undergoing convergent extension. This cell shortens from a length of 47 μm to a length of 42 μm, likely due to retraction of a protrusion (arrow). Scale bar is 30 μm.

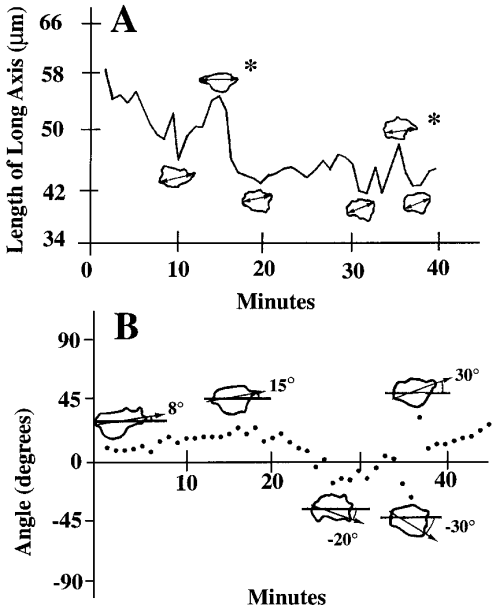

FIG. 7. (A) The length of a cell's long axis is plotted as a function of time, and corresponding diagrams of the cell at various times are shown. Such plots were used to count episodes of cell elongation. An episode of cell elongation is defined as a trough-to-peak rise greater than 4 μm. Lines with double arrows indicate the cell's long axis. The cell is elongated at peaks (asterisks) in the plot and is isodiametric in the valleys. In this particular trace the cell has two episodes of elongation. (B) The angle of orientation of the long axis of the cell relative to the mediolateral axis of the explant is plotted as a function of time, and corresponding diagrams show the cell shape at various times. The arrows within the diagrams of the cells indicate the long axis. Thick lines on each cell indicate the mediolateral axis of the explant.

lamelliform protrusions in many other directions (Fig. 8). Counting all neural deep cells' protrusions and scoring their angular distribution demonstrated that this protrusive activity is indeed mediolaterally biased. Forty-eight percent of all neural deep cells' protrusions (new and successive advances) were within 30° of the mediolateral axis (Fig. 9). This is a significantly greater percentage than the 33% expected to be mediolaterally oriented in a uniform distribution ($P < 0.01$, Rayleigh's test). Although some heterogeneity existed among our sample of neural deep cells in the extent to which cells had mediolaterally biased protrusive activity, 70% of the cells we observed had more than 40% of their protrusions mediolaterally oriented. We conclude that, on average, the neural deep cells show mediolaterally biased protrusive activity.

The neural deep cell bias in protrusive activity could be due to cells advancing more new protrusions mediolaterally, as well as to their mediolateral protrusions undergoing more successive advances once they are extended (being more persistent). Our observation that during the advance of a single mediolateral protrusion, neural cells continuously advanced and retracted numerous small protrusions in many other directions suggests that their mediolateral protrusions undergo more successive advances (Fig. 8). To investigate this issue we classified the advances of neural deep cells' protrusions as new or successive advances (see Materials and Methods) and then scored the angular distributions of these two types of advances ($n = 17$ cells, four explants). As expected, successive advances were mediolaterally biased; 53% of all successive advances were mediolaterally oriented. New advances, however, were also mediolaterally biased, with 48% of all new advances mediolaterally oriented (Table 2). Thus, neural deep cells both advance more new protrusions mediolaterally and exhibit more successive advances in their mediolateral protrusions, both of which imply that their mediolateral protrusions are important in generating traction for intercalation.

Although neural and mesodermal cells both exhibit mediolaterally biased protrusive activity, at this level of resolution the mesodermal cells do not show the background ''noise'' of small protrusions in other directions that the neural cells exhibit. This difference in motility is evident in their protrusion rates: Neural cells on average advance 24 new protrusions per hour, whereas mesodermal cells advance 7 new protrusions per hour (Table 2). However, because approximately half of the neural cells' protrusions are mediolaterally oriented, while more than 70% of the mesodermal cells' protrusions are mediolaterally oriented, the two cell types show more comparable mediolateral protrusion rates (Table 2).

Neural Deep Cells Show Directional Protrusive Activity

A significant fraction of the neural cells we examined in higher magnification videos exhibited a preferred direction of protrusive activity. Seven out of 12 mediolaterally biased cells exhibited unbalanced protrusive activity with 4 of the 7 cells advancing more protrusions medially than laterally (Fig. 10A) and the remaining 3 advancing more protrusions laterally. (Handedness of cells was taken into account in these measurements.) Most of these cells were sampled for times ranging between 70 and 100 min, implying that neural deep cells may sustain directional protrusive activity over substantial periods of time (Fig. 10A). Several nonmediolaterally biased cells also exhibited a preferred direction of protrusive activity, as illustrated by the plot in Figure 10B. These data suggest that neural deep cells can exhibit directional protrusive activity, in contrast to the mesodermal cells, whose protrusive activity appears more continuously balanced in the medial and lateral directions.

These data also indicate that some heterogeneity in motility was present within the neural deep cells. However, our explants and sample size were not large enough to determine whether this heterogeneity represented patterning in

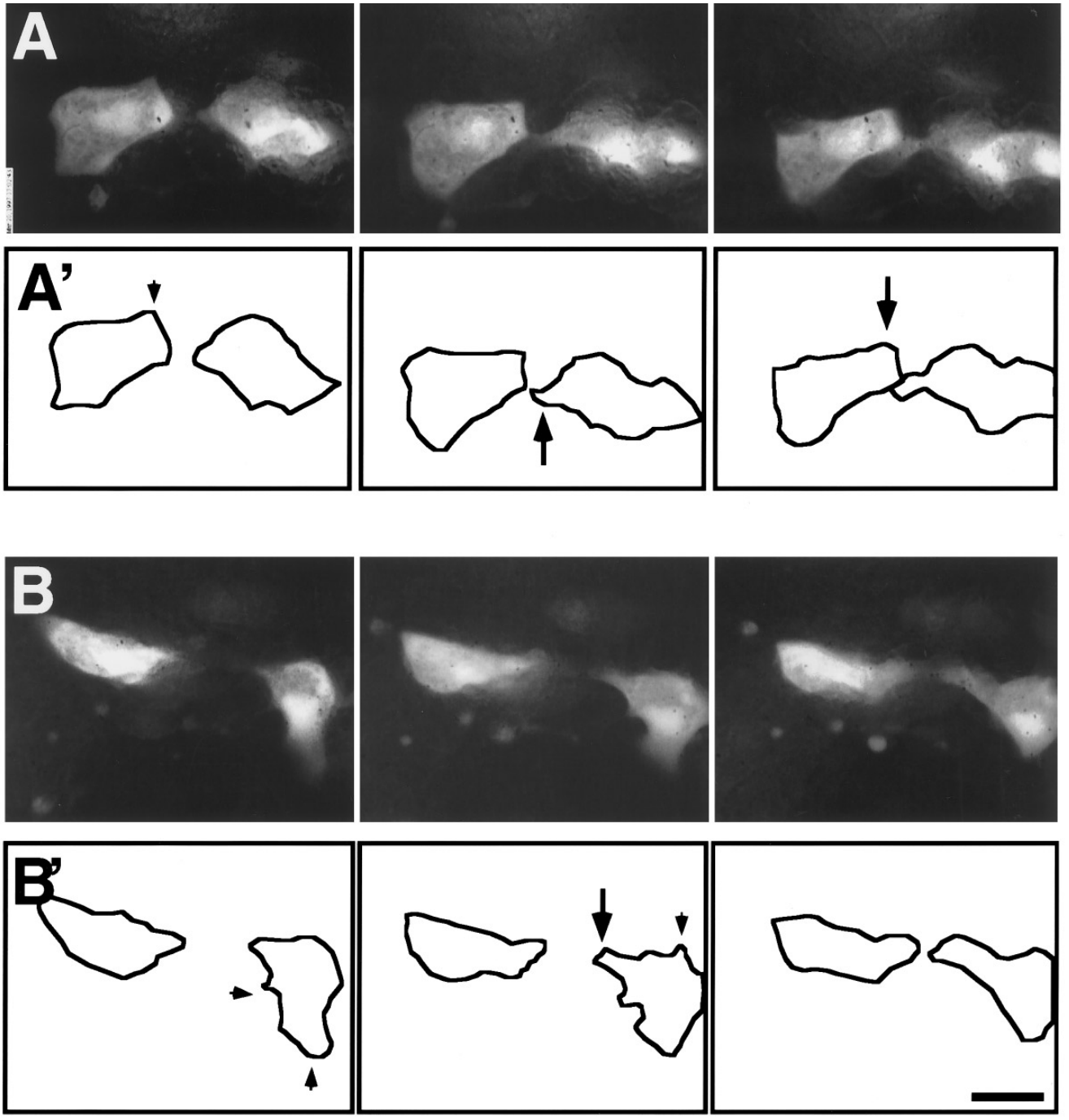

FIG. 8. Stills taken from a higher magnification time-lapse video (×60) (A, B), and corresponding tracings (A′, B′), show sequential images of cells in a neural deep cell explant undergoing convergent extension. (A, A′) Both cells extended mediolaterally oriented protrusions during the time period shown here. Note that cells became more mediolaterally elongated as they extended mediolateral protrusions. Cells also extended and retracted small protrusions in other directions during this time period. (B, B′) The cell on the right extended a mediolaterally oriented protrusion while retracting several non-mediolaterally oriented protrusions, including a large posteriorly directed protrusion. Large arrows indicate mediolaterally oriented protrusions. Small arrows indicate non-mediolaterally oriented protrusions. The anteroposterior axis of the explant is vertically oriented, with anterior at the top of the images. Images are 6 min apart in (A, A′) and 4 min apart in (B, B′). Scale bar is 40 μm.

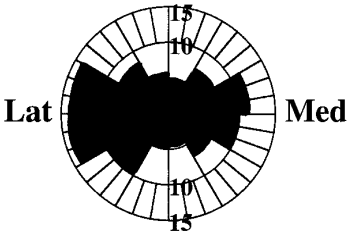

FIG. 9. The angular distribution of advances of protrusions of neural deep cells during convergent extension was calculated from both low and higher magnification time-lapse videos. Advances of both new and previously existing protrusions were counted for a sample of 39 cells in 7 explants (1 or more cells per explant). 48% of all advances of these cells were within 30° of the mediolateral axis of the explant. The mediolateral axis is indicated in the plot. Lat, lateral; Med, medial. Numbers on vertical axis represent percentages.

the neural deep tissue or merely random variation in cell motility.

DISCUSSION

In this paper we showed that single-layered neural deep cell explants taken from *X. laevis* late gastrula embryos converge and extend autonomously. These explants narrow mediolaterally and elongate anteroposteriorly, independent of physiological or mechanical contact with neighboring tissues. Convergent extension of neural deep cell explants occurs by cells actively mediolaterally intercalating, with little contribution from cell shape changes and cell division. We described the cell motility that underlies neural deep cell intercalation, using time-lapse videomicroscopy of fluorescently labeled cells in neural deep cell explants. In these videos we observed that neural deep cells exhibit mediolaterally biased protrusive activity which is expressed in an episodic manner and can be directional. These descriptions of the active cell motility underlying neural convergent extension in *X. laevis* are the first high-resolution video documentation of cell motility underlying neural convergent extension in any system. Additionally, the neural deep cell explant that we developed is an accessible *in vivo* tissue system conducive to further investigation of issues in *Xenopus* neural morphogenesis, including patterning, induction and cell motility. We now discuss the implications of the findings described in this paper.

Neural Deep Cells Converge and Extend Autonomously

Explants consisting of a single layer of neural deep cells converge and extend autonomously. Similarly, Shih and Keller previously showed that explants of mesodermal deep cells converge and extend autonomously (Shih and Keller, 1992a). Both mesodermal and neural deep cells then likely contribute force for convergent extension of the dorsal region of the embryo *in vivo*. By comparing the stiffness, amount of force produced, and temporal course of force production by each of these two tissues (Moore *et al.*, 1995) we will be able to evaluate their relative contributions and gain further insight into the cellular biomechanics of convergent extension. Preliminary data on these issues is available from experiments measuring the force exerted by Keller sandwiches during convergent extension. In these experiments, the mesodermal tissue overpowered the neural tissue (Moore *et al.*, 1995), suggesting that the neural tissue exerts less force or is less stiff than the mesodermal tissue.

Do other vertebrate neural plates undergo autonomous convergent extension and exhibit cell behaviors similar to the *Xenopus* deep cell behaviors? Most of these other vertebrate neural plates, such as those of amniotes and newts, consist of a single layer of epithelial cells (Jacobson and Gordon, 1976; Schoenwolf and Smith, 1990). Because epithelial cells possess more intercellular adhesive junctions than deep cells (Fristrom, 1988), these neural epithelial systems may be unable to actively rearrange as the *Xenopus* deep cells do. Moreover, epithelial cells are restricted to extending protrusions basal-laterally, rather than on all faces as deep cells do. In support of these ideas, we have not observed protrusive activity among the *Xenopus* neural epithelial cells similar to that we described for the deep cells (Keller *et al.*, 1992a) nor have we observed these cells to converge and extend autonomously (Keller and Danilchik, 1988). However, the neural plate of the California newt does undergo convergent extension autonomously (Jacobson and Gordon, 1976), apparently driven by protrusions along the lateral edges of the neural epithelial cells (Jacobson *et al.*, 1986). Unfortunately, no other neural epithelial systems have been examined for protrusive activity and autonomous

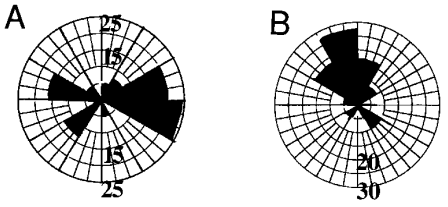

FIG. 10. Angular distributions of protrusions for two individual neural deep cells are shown. (A) This cell exhibited a medial directional bias (mean angle = 12°) during the 150 min it was observed. Rayleigh's test confirmed that distribution was nonuniform ($P < 0.05$) (B) This cell did not exhibit mediolaterally biased protrusive activity but clearly had a preferred direction of protrusive activity (mean angle = 90°) during the 120 min it was observed. Again, Rayleigh's test confirmed that distribution was nonuniform ($P < 0.0001$). The mediolateral axis is as indicated in Fig. 9. Numbers on vertical axes represent percentages.

convergent extension. Our work hopefully will serve as a starting point for the examination of these other systems, such as amniotes.

Neural Deep Cells Mediolaterally Intercalate without Changing Shape

Throughout most of the process of convergent extension, the neural deep cells mediolaterally intercalate without undergoing a progressive change in shape. In contrast, the mesodermal cells progressively elongate mediolaterally (and presumably shorten anteroposteriorly) concomitantly with their mediolateral intercalation (Shih and Keller, 1992a). Based on this difference in cell shape change we predict that a given amount of intercalation will result in greater extension for the neural deep cells than for the mesodermal cells. Our prediction is consistent with data presented by Keller and Danilchik (1989) indicating that in the Keller sandwich explant, the neural ectoderm converges and extends more than the mesoderm region. The different shape changes shown by the neural and mesodermal cells reflect their disparate fates; the mesodermal cells elongate as part of their program of differentiation into notochord and somitic cells, both of which are elongated in the plane of intercalation (Wilson *et al.*, 1989). Neural cells eventually elongate as well (columnarize) (Burnside and Jacobson, 1968) but do so perpendicular to the plane of mediolateral intercalation. These differences in shape change may also reflect differences in protrusive activity shown by neural and mesodermal cells, discussed below.

The Mechanism of Neural Convergent Extension: Oriented Protrusive Activity Drives Mediolateral Cell Intercalation

A major goal of this study was to determine the motility underlying mediolateral intercalation of neural deep cells. Time-lapse videos of neural deep cell motility during convergent extension showed that most cells exhibit mediolaterally biased protrusive activity, which appears to be the predominant type of anisotropic protrusive activity exhibited by neural deep cells. We propose that neural deep cells intercalate by applying their mediolaterally oriented protrusions onto adjacent cells, exerting traction on these cells and pulling themselves between one another using this traction. Mesodermal cells also exhibit mediolaterally biased protrusive activity during their convergent extension (Shih and Keller, 1992a). Accordingly, the mechanism of mediolateral intercalation we propose for neural deep cells is similar to the mechanism we previously described for mesodermal cells (Shih and Keller, 1992a; Keller *et al.*, 1991). The fact that both neural and mesodermal cells exhibit mediolaterally biased protrusive activity establishes a trend in the mechanism of convergent extension by mediolateral cell intercalation. However, it is too premature to suggest that mediolateral bias in protrusive activity is a universal component of convergent extension by mediolateral cell intercalation since neural and mesodermal tissues are the only two examples studied at this level of detail thus far. Our study of the neural deep cell motility underlying convergent extension thus highlights the need for resolving the cell behavior of the other examples of convergent extension by mediolateral intercalation (mentioned in the Introduction).

Although neural and mesodermal cells both appear to generate traction for intercalation by mediolateral protrusive activity, differences in their expression of this protrusive activity bring to mind two models we previously proposed for how traction generated by protrusive activity drives cell intercalation (Keller *et al.*, 1991). The mesodermal cells show a relatively constant protrusive activity at their medial and lateral ends (Shih and Keller, 1992a). The model that best fits this behavior suggests that cells generate constant, balanced traction by frequent protrusions on their medial and lateral ends. Using this traction, cells gradually advance between one another, intercalating in a relatively constant movement (Fig. 11A). The neural deep cells, on the other hand, exhibit episodic mediolateral protrusive activity that distorts their shape in a corresponding episodic manner. According to the model which best fits this behavior, cells first crawl on one another, elongating as they crawl (Figs. 11B and 11C). Neural cells may crawl on one another bidirectionally (Fig. 11B), as the mesodermal cells do, or directionally (Fig. 11C). In either case, when these cells reach some limit of stretch, they contract, shortening and pulling themselves between one another (Figs. 11B and 11C). Note that in the model describing the neural tissue, cells move past one another during the contraction and shortening phase, whereas in the mesodermal model cells intercalate continuously.

Induction and Patterning of Neural Deep Cell Behaviors

We propose that convergent extension of neural deep cells is induced by planar signals from Spemann's organizer, with vertical signals playing a secondary, if any, role in this induction. Keller and others (1992b) demonstrated that planar signals from the mesoderm are sufficient to induce convergent extension in sandwich explants (epithelial and deep cells). Earlier experiments of Keller and Danilchik (1988) investigating induction of neural deep cell convergent extension, however, were less equivocal. Although the neural region of these deep cell explants underwent convergent extension, they did not show that vertical signals were absent. Moreover, our neural deep cell explants were made at the late mid-gastrula stage, after having substantial planar and vertical contact with the mesoderm. One interpretation of these results is that vertical signals act in synergy with planar signals, the two signals together inducing more convergent extension than either one alone (Dixon and Kintner, 1989). Alternately, planar signals may be sufficient to induce convergent extension of neural deep cells. Neural deep

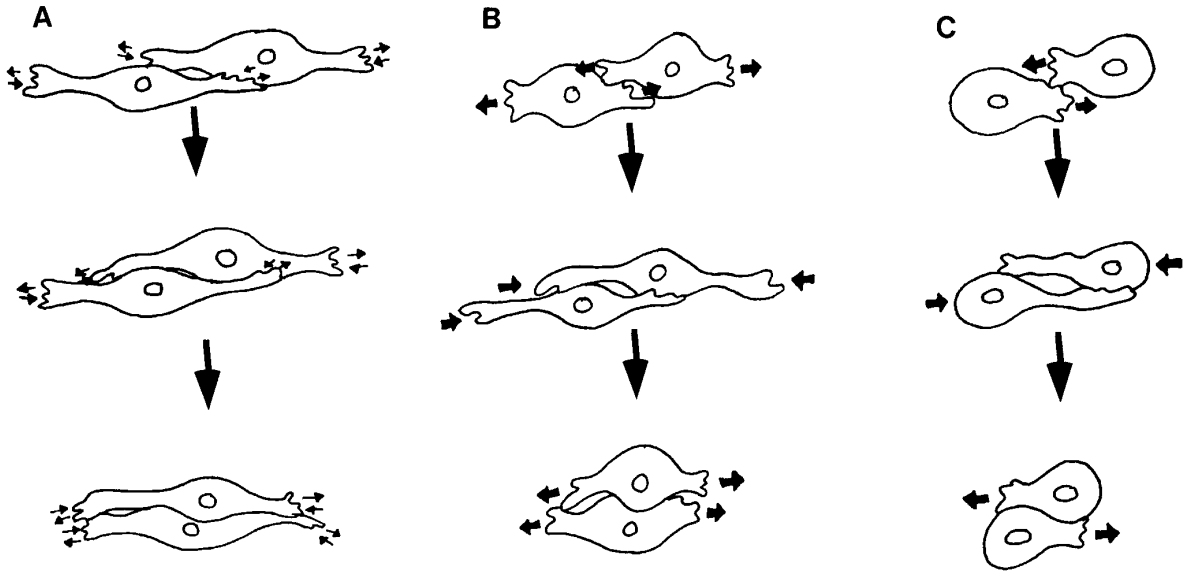

FIG. 11. Model for how differences in mesodermal (A) and neural (B, C) mediolateral protrusive activity could result in different mechanisms of intercalation. (A) Mesodermal cells continuously exert protrusive activity, without apparent change in cell shape as they do so. They continuously generate traction with these protrusions, progressively moving past one another. (B, C) The neural cells, on the other hand, undergo episodes of protrusive activity, repeatedly elongating and shortening as a result. They extend protrusions either bidirectionally (B) or unidirectionally (C), apply these protrusions onto adjacent cells, and exert traction. They then contract, shorten, and pull themselves between one another, now ready for another episode of intercalation.

cells may require time, rather than vertical signals, for their convergent extension to become organized and robust enough to be autonomous.

Although we observed heterogeneity in motility among the neural deep cells, our explants and sample sizes were not large enough to determine whether this variation in motility was regional or random. Some cells had medially or laterally directed protrusive activity, others had mediolaterally balanced protrusive activity, still others had nonmediolaterally biased protrusive activity. We propose two possible mechanisms that could underlie regional variation in motility in the neural tissue: (1) Many genes are expressed as anteroposterior stripes in the neural plate during the late gastrula stages (Espeseth *et al.*, 1995). A number of such stripes could delimit subdomains in the neural plate by functioning as restrictive boundaries; perhaps cells move freely medially or laterally between the stripes but are unable to traverse them. (2) A graded signal may be present in the neural tissue, with cells crawling toward the region of maximum signal. If cells were crawling toward the midline we would expect cells located farther laterally to have medially directed protrusive activity and those at the midline to have more balanced protrusive activity.

Persistent vertical signals from Spemann's organizer beyond stage 11.5 will likely induce (more) regional variations in the cell behaviors underlying neural ectoderm convergent extension. Regional differentiations of the neural plate, such as formation of the floorplate and columnarization and wedging of deep cells, require persistent vertical interactions with the underlying mesoderm tissues beyond the late mid-gastrula stage (Poznanski *et al.*, 1997), as is the case in other vertebrates (Placzek *et al.*, 1990; Yamada *et al.*, 1993). Cell behaviors underlying convergent extension may be altered along with such regional differentiations. Jacobson has shown that protrusive activity of newt neural epithelial cells is inhibited at the notoplate/neural plate boundary (Jacobson *et al.*, 1986). Protrusive activity of *Xenopus* neural deep cells may be inhibited in a similar manner at the notoplate/neural plate boundary. We have observed such a boundary in neural deep cell explants that have persistent vertical signals beyond stage 11.5 and are presently investigating whether there is any variation in neural deep cell protrusive activity associated with this boundary.

ACKNOWLEDGMENTS

We thank members of the Keller and Koehl labs (past and present) for stimulating, entertaining discussion and moral support. We thank Dr. Connie Lane for help with experiments, Dr. Lance Davidson for providing computer support, and Anna Edlund for comments on the manuscript. We are grateful to Richard Harland for providing us with the N-CAM antibody. This work was supported

by NIH Grant HD25595 to Ray Keller. Tamira Elul is supported by a HHMI predoctoral fellowship.

REFERENCES

Bolce, M. E., Hemmati-Brivanlou, A., Kushner, P. D., and Harland, R. M. (1992). Ventral ectoderm of *Xenopus* forms neural tissue, including hindbrain, in response to activin. *Development* **115,** 681–688.

Burnside, B., and Jacobson, A. (1968). Analysis of morphogenetic movements in the neural plate of the newt *Taricha torosa*. *Dev. Biol.* **18,** 537–552.

Condic, M. L., Fristrom, D., and Fristrom, J. W. (1991). Apical cell shape changes during *Drosophila* imaginal leg disc elongation: A novel morphogenetic mechanism. *Development* **111,** 23–33.

Dixon, J., and Kintner, C. R. (1989). Cellular contacts required for neural induction in *Xenopus* embryos: evidence for two signals. *Development* **106,** 749–757.

Domingo, C., and Keller, R. (1995). Induction of notochord cell intercalation behavior and differentiation by progressive signals in the gastrula of *Xenopus laevis*. *Development* **121,** 3311–3321.

Eagleson, G. W., and Harris, W. A. (1990). Mapping of the presumptive brain regions in the neural plate of *Xenopus laevis*. *J. Neurobiol.* **21,** 427–440.

Espeseth, A., Johnson, E., and Kintner, C. (1995). *Xenopus* F-cadherin, a novel member of the cadherin family of cell adhesion molecules, is expressed at boundaries in the neural tube. *Mol. Cell Neurosci.* **6,** 199–211.

Ettensohn, C. (1985). Gastrulation in the sea urchin embryo is accompanied by the rearrangement of invaginating epithelial cells. *Dev. Biol.* **112,** 383–390.

Fristrom, D. (1988). The cellular basis of epithelial morphogenesis: a review. *Tissue and Cell* **20(5),** 645–690.

Gould, S. E., and Grainger, R. M. (1997). Neural induction and anteroposterior patterning in the amphibian embryo: past, present, and future. *Cell. Mol. Life Sci.* **53,** 319–338.

Gurdon, J. (1977). Methods for nuclear transplantation in amphibia. *Methods Cell Biol.* **16,** 125–139.

Hardin, J., and Cheng (1986). The mechanisms and mechanics of archenteron elongation during sea urchin gastrulation. *Dev. Biol.* **115,** 490–501.

Harris, W., and Hartenstein, V. (1991). Neuronal determination without cell division. *Neuron* **6,** 499–515.

Hartenstein, V. (1989). Early neurogenesis in *Xenopus:* The spatiotemporal pattern of proliferation and cell lineages in the embryonic spinal cord. *Neuron* **3,** 399–411.

Hemmati-Brivanlou, A., and Melton, D.-G. (1997). Vertebrate embryonic cells will become nerve cells unless told otherwise. *Cell* **88,** 13–17.

Irvine, K., and Wiechaus, E. (1994). Cell intercalation during *Drosophila* germband extension and its regulation by pair-rule segmentation genes. *Development* **120,** 827–841.

Jacobson, A. (1978). Some forces that shape the nervous system. *Zoon* **6,** 13–21.

Jacobson, A. G. (1981). Morphogenesis of the neural plate and tube. *In* ''Morphogenesis and Pattern Formation'' (T. G. Connelly, L. L. Brinkley, and B. M. Carlson, Eds.), pp. 233–263. Raven Press, New York.

Jacobson, A. G., and Gordon, R. (1976). Changes in the shape of the developing vertebrate nervous system analyzed experimentally, mathematically, and by computer simulation. *J. Exp. Zool.* **197,** 191–246.

Jacobson, A. G., and Moury, J. D. (1995). Tissue boundaries and cell behavior during neurulation. *Dev. Biol.* **171,** 98–110.

Jacobson, A. G., Oster, G. F., Odell, G. M., and Cheng, L. Y. (1986). Neurulation and the cortical tractor model for epithelial folding. *J. Embryol. Exp. Morphol.* **96,** 19–49.

Kay, B., and Peng, B. (1991). ''*Xenopus laevis:* Practical Uses in Cell and Molecular Biology.'' Academic Press, San Diego.

Keller, R. (1991). Early embryonic development of *Xenopus laevis*. *Methods Cell Biol.* **36,** 61–113.

Keller, R., and Danilchik, M. (1988). Regional expression, pattern and timing of convergence and extension during gastrulation of *Xenopus laevis*. *Development* **103,** 193–209.

Keller, R., Poznanski, A., and Elul, T. (1996). Experimental embryological methods for analysis of neural induction in the amphibian. *In* ''Methods in Molecular Biology: Molecular Embryology: Methods and Protocols'' (P. Sharpe and I. Mason, Eds.). Humana Press, Totowa, NJ.

Keller, R., Shih, J., and Sater, A. (1992a). The cellular basis of the convergence and extension of the *Xenopus* neural plate. *Dev. Dyn.* **193,** 199–217.

Keller, R., Shih, J., Sater, A. K., and Moreno, C. (1992b). Planar induction of convergence and extension of the neural plate by the organizer of *Xenopus*. *Dev. Dyn.* **193,** 218–234.

Keller, R., Shih, J., Wilson, P., and Sater, A. (1991). Pattern and function of cell motility and cell interactions during convergence and extension in Xenopus. *In* ''Cell Interactions in Early Development.'' Wiley-Liss, New York.

Keller, R., and Tibbetts, P. (1989). Mediolateral cell intercalation in the dorsal, axial mesoderm of *Xenopus laevis*. *Dev. Biol.* **131,** 539–549.

Keller, R. E. (1975). Vital dye mapping of the gastrula and neurula of *Xenopus laevis*. I. Prospective areas and morphogenetic movements of the superficial layer. *Dev. Biol.* **42,** 222–241.

Keller, R. E. (1976). Vital dye mapping of the gastrula and neurula of *Xenopus laevis*. II. Prospective areas and morphogenetic movements of the deep layer. *Dev. Biol.* **51,** 118–137.

Keller, R. E. (1978). Time-lapse cinemicrographic analysis of superficial cell behavior during and prior to gastrulation in *Xenopus laevis*. *J. Morphol.* **157,** 223–248.

Kintner, C. R., and Brockes, J. P. (1984). Monoclonal antibodies identify blastemal cells derived from dedifferentiating limb regeneration. *Nature* **308,** 67–69.

Kushner, P. D. (1984). A library of monoclonal antibodies to Torpedo cholinergic synaptosomes. *J. Neurochem.* **43,** 775–786.

Moore, S. W., Keller, R. E., and Koehl, M. A. (1995). The dorsal involuting marginal zone stiffens anisotropically during its convergent extension in the gastrula of *Xenopus laevis*. *Development* **121,** 3131–3140.

Nieuwkoop, P., and Faber. (1967). ''Normal Table of *Xenopus laevis* (Daudin).'' North–Holland, Amsterdam.

Nieuwkoop, P., and Florshutz, P. A. (1950). Quelques caracteres speciaux de la gastrulation et de la neurulation de l'oeuf de *Xenopus laevis,* Daud. et de quelques autres Anoures. 1ere partie.- Etude descriptive. *Arch. Biol.* **61,** 113–150.

Placzek, M., Tessier-Lavigne, M., Yamada, T., Jessell, T., and Dodd, J. (1990). Mesodermal control of neural cell identity: Floor plate induction by the notochord. *Science* **250,** 985–988.

Poznanski, A., and Keller, R. (1997). The role of planar and early

vertical signaling in patterning the expression of Hoxb-1 in *Xenopus. Dev. Biol.* **184,** 351–366.

Poznanski, A., Minsuk, S., Stathopoulos, D., and Keller, R. (1997). Epithelial cell wedging and neural trough formation are induced planarly in *Xenopus,* without persistent vertical interactions with mesoderm. *Dev. Biol.,* in press.

Sater, A. K., Steinhardt, R. A., and Keller, R. (1993). Induction of neuronal differentiation by planar signals in *Xenopus* embryos. *Dev. Dyn.* **197,** 268–280.

Schoenwolf, G. C., and Alvarez, I. S. (1989). Roles of neuroepithelial cell rearrangement and division in shaping of the avian neural plate. *Development* **106,** 427–439.

Schoenwolf, G. C., and Smith, J. L. (1990). Mechanisms of neurulation: Traditional viewpoint and recent advances. *Development* **109,** 243–270.

Schoenwolf, G. C., and Yuan, S. (1995). Experimental analyses of the rearrangement of ectodermal cells during gastrulation and neurulation in avian embryos. *Cell Tissue Res.* **280,** 243–251.

Shih, J., and Keller, R. (1992a). Cell motility driving mediolateral intercalation in explants of *Xenopus laevis. Development* **116,** 901–914.

Shih, J., and Keller, R. (1992b). Patterns of cell motility in the organizer and dorsal mesoderm of *Xenopus laevis. Development* **116,** 915–930.

Trinkaus, J. P., Trinkaus, M., and Fink, R. D. (1992). On the convergent cell movements of gastrulation in *Fundulus. J. Exp. Zool.* **261,** 40–61.

Warga, R. M., and Kimmel, C. B. (1990). Cell movements during epiboly and gastrulation in zebrafish. *Development* **108,** 569–580.

Wilson, P. A., Oster, G., and Keller, R. (1989). Cell rearrangement and segmentation in Xenopus: direct observation of cultured explants. *Development* **105,** 155–166.

Yamada, T., Pfaff, S. L., Edlund, T., and Jessell, T. M. (1993). Control of cell pattern in the neural tube: Motor neuron induction by diffusible factors from notochord and floor plate. *Cell* **73,** 673–686.

Zar, J. H. (1974). ''Biostatistical Analysis.'' Prentice Hall, Englewood Cliffs, NJ.

Received for publication May 14, 1997
Accepted August 5, 1997